MODIS time series contribution for the estimation of nutritional properties of alpine grassland

Luigi Ranghetti[1,2,*], Bruno Bassano[3], Giuseppe Bogliani[2], Alberto Palmonari[4], Andrea Formigoni[4], Laura Stendardi[5] and Achaz von Hardenberg[3,6]

[1] Institute for Electromagnetic Sensing of the Environment, Consiglio Nazionale delle Ricerche, Via Corti 12, 20133 Milano, Italy

[2] Department of Earth and Environmental Sciences, Università di Pavia, Via Ferrata 9, 27100 Pavia, Italy

[3] Alpine Wildlife Research Centre, Parco Nazionale Gran Paradiso, Fraz. Dégioz 11, 11010 Valsavarenche (AO), Italy

[4] Department of Veterinary Medicine, Università di Bologna, Via Tolara di Sopra 50, 40064 Ozzano dell'Emilia (BO), Italy

[5] Department of Agri-Food Production Sciences and the Environment, Università di Firenze, Via delle Cascine 5, 50144 Firenze, Italy

[6] Department of Biological Sciences, University of Chester, Parkgate Road, Chester, CH1 4BJ, United Kingdom

[*] Corresponding author, e-mail address: ranghetti.l@irea.cnr.it

Abstract

Despite the Normalised Difference Vegetation Index (NDVI) has been used to make predictions on forage quality, its relationship with bromatological field data has not been widely tested. This relationship was investigated in alpine grasslands of the Gran Paradiso National Park (Italian Alps). Predictive models were built using remotely sensed derived variables (NDVI and phenological information computed from MODIS) in combination with geo-morphometric data as predictors of measured biomass, crude protein, fibre and fibre digestibility, obtained from 142 grass samples collected within 19 experimental plots every two weeks during the whole 2012 growing season. The models were both cross-validated and validated on an independent dataset (112 samples collected during 2013). A good predictability ability was found for the estimation of most of the bromatological measures, with a considerable relative importance of remotely sensed derived predictors; instead, a direct use of NDVI values as a proxy of bromatological variables appeared not to be supported.

Keywords

NDVI, MODIS, time series, nutritional quality, biomass, grassland, Alps.

Introduction

The variability in nutrient content of pastures over time is of key importance in understanding the population dynamics of herbivores relying on grasslands as their only food resource. Normalised Difference Vegetation Index (NDVI) [Rouse et al., 1974] is widely used to monitor vegetation and plant responses to environmental change [Pettorelli et al., 2011]. NDVI is directly related to the fraction of absorbed photosynthetic active radiation intercepted (fAPAR) both theoretically [Sellers et al., 1992; Myneni and Williams, 1994] as well in the field [e.g. Di Bella et al., 2004; Viña and Gitelson, 2005; Richardson et al., 2007; Gitelson et al., 2014], in particular within herbaceous environments such as grasslands [e.g. Moreau et al., 2003; Fensholt et al., 2004; Boschetti et al., 2007; Li et al., 2010]. The correlation of NDVI with other characteristics of the canopy is only indirect, and needs to be empirically tested for different sensors and cover types [Roberts, 2001]. Biomass and Leaf Area Index (LAI) are probably the physical parameters which have been tested more in a large number of different environments: forests [e.g. González-Alonso et al., 2006; Tan et al., 2007; Madugundu et al., 2008], rice fields [e.g. Casanova et al., 1998; Wang et al., 2007; Gnyp et al., 2014], dry crops [e.g. Quarmby et al., 1993; Thenkabail et al., 2000; Marti et al., 2007; Boschetti et al., 2009] and extensive herbaceous lands [e.g. Moreau et al., 2003; Wang et al., 2005; Beeri et al., 2007; Darvishzadeh et al., 2008]. The relationship between NDVI and chemical parameters such as nitrogen content or digestibility has been tested only in few cases instead, and the lack of field validations of this relationship casts doubts on the usability of NDVI as a standalone estimator of forage quality [Pettorelli et al., 2011]. Islam et al. [2011] reported a high correlation between NDVI and nitrogen content of maize plants, but only at one specific phenological stage (8-leaf stage). Other studies linked NDVI with faecal crude protein (FCP) of large herbivores, which is considered a reliable indicator of the quality of vegetation [Cordova et al., 1978; Leslie and Starkey, 1985; Hodgman et al., 1996]. For example, Ryan et al. [2012] showed a positive relationship between log transformed NDVI and nitrogen faecal content of African Buffalo (*Syncerus caffer*) and Hamel et al. [2009] found a negative relationship between integrated NDVI in

June and the date of the peak in FCP of mountain goats (*Oreamnos americanus*) and bighorn sheep (*Ovis canadensis*). Other studies used NDVI as a proxy of nutritional content of grasslands without validating it with field measures [Griffith et al., 2002; Boone et al., 2006; Pettorelli et al., 2007; Mueller et al., 2008].

Another requirement in using remotely sensed data, besides field validation, is that spatial resolution should be adequate to recognise the surveyed surface, in order to reduce the presence of mixed pixels, which could lead to wrong estimations of parameters. For example, this may be an issue if estimations of grass biomass are done for pixels which contain also woodland [Elvidge and Lyon, 1985; Huete et al., 1985; Huete and Tucker, 1991].

Moderate Resolution Imaging Spectroradiometer (MODIS) data is probably the most widely used satellite data for phenological analyses, since its daily temporal resolution allows to reconstruct temporal profiles of vegetation indices, and its fifteen years long time series permits to explore changes of phenological parameters over time [Pettorelli et al., 2005; Boschetti et al., 2009]. The spatial resolution of MODIS (250 m for red and NIR bands; 500 m or 1 km for other bands) is sufficiently detailed for extensive high altitude grasslands such as those found on the Tibetan plateau and other mountain areas of China, characterised by large extensions and high homogeneity; indeed, most of the studies which use MODIS data to estimate forage quality in alpine grassland environments have been conducted in these sites [e.g. Zha et al., 2005; Gao et al., 2009; Zhang et al., 2011; Mao et al., 2012; Cong et al., 2013; Liang et al., 2013; Zhang et al., 2013; Xu et al., 2014]. Instead, in the European Alps, grasslands are typically located in the alpine zone, which is generally fragmented between lower woody and higher rocky habitats, with a consequent higher spatial heterogeneity (at these elevations large uplands are uncommon, especially in the Western Alps). The high heterogeneity of grasslands in the European Alps entails that pure grassland 250 m pixels tend to be enclosed by mixed pixels, adding noise to the estimates when using NDVI as the only predictor of the nutritional content of pastures.

Being able to reliably estimate changes in the nutritional value of alpine grasslands over the last decades might be critical for better understanding the population dynamics of alpine herbivores. The case of the population of Alpine ibex (*Capra ibex*) in the Gran Paradiso National Park (GPNP, Northwester Italian Alps) is particularly emblematic: the dynamics of the population, estimated from total counts performed by park wardens since 1956 [von Hardenberg et al., 2000], was well explained up to 20 years ago by the interaction between winter snow depth and population density [Jacobson et al., 2004]. However, deterministic models fail to predict the decline in the population from nearly 5000 individuals counted in 1993 to little more than the 2300 counted in 2009 even when including in the models information on the age structure of the population [Mignatti et al., 2012]. Pettorelli et al. [2007] suggested that changes in the phenology and in forage quality due to climate change are negatively related to Alpine ibex kid survival and thus to the decline in the total population due to lack of recruitment. However, Pettorelli et al. [2007] based this hypothesis on the simple correlation between a crude NDVI-based indicator (NDVImax, estimated on 1×1 km squares and averaged over the whole territory of the GPNP) and yearly estimates of Alpine ibex kids survival. An estimation of the nutritional content of Alpine pastures in the GPNP made by calibrating a model with ground references would permit to more thoroughly investigate the interaction between climate change, grassland phenology, forage quality and the dynamics of the Alpine ibex population. The aim of this study is thus to assess the contribution of remotely sensed predictors from MODIS NDVI time series combined with geo-morphometric information to estimate the nutritional content of forage in Alpine grassland characterised by high environmental heterogeneity.

Methods

Study area

All field data have been collected within the territory of the GPNP (45.40° – 45.65° N, 7.07° – 7.58° E). The morphology of this area is typical of western Italian Alps, with high altitudinal ranges:

valley bottoms are located between 1000 and 2000 m, while ridges rarely are at less than 3000 m (the highest altitude is reached at 4061 m, at the top of Gran Paradiso). Grasslands are located in the middle part, in the alpine zone (2200-2700 m), between woodlands and snow habitats (rocks, screes and glaciers): for this reason grassland surface appears very fragmented. Also the lithological composition of the area is quite heterogeneous, due to the presence of both calcareous and siliceous formations (calcschist ophiolite units – which are present mainly in the western part of the GPNP – define a mosaic of acid and basic soils, while granite gneisses – found mostly in the eastern part – are mainly acid). This condition, together with the heterogeneity in the exposure of mountainsides (mainly South in the southern part and East or West in the northern, but very variable due to the presence of a lot of deep small valleys), contributes to the presence of diversified plant communities.

Field data

Field data were collected during the 2012 growing season within 19 experimental plots, the maximum number of plots which one single operator can sample within the given time interval (see Figure 1 and Figure 2 for details). These plots have been chosen within GPNP alpine grasslands taking into account the following restrictions: (i) a minimum distance of 500 m from woodland, to avoid the possible interaction of this surface in the determination of the NDVI pixel value; (ii) a minimum distance of 1 km between plots, to minimise the autocorrelation between MODIS values; (iii) a balanced coverage of the altitudinal range of the grasslands and of the different exposures.

[Figure 1 about here]

[Figure 2 about here]

Each plot is composed of a squared surface of 3 × 3 m, enclosed to prevent grazing from domestic and wild herbivores. Enclosures were located on a homogeneous surface, enough representative of the surrounding buffer of 300 m (in terms of exposure, slope and microhabitat). Data collection was done from the beginning of the growing season (second half of May – end of June, depending on the plot) to the end of September (when all the vegetation communities in the plots reached senescence), with an interval between consecutive samples of two weeks. With this experimental

129 design a total of 142 samples was obtained (from 4 to 10 samples for each plot). Each plot was
130 divided into sectors of 50 × 50 cm; during each sampling session, all the grass present in one of
131 these sectors was cut (with the exception of the eventual dry grass remaining from the year before).
132 Also, a 1 × 1 m surface was reserved to take, each time, measures about grass height (taking 16
133 measures into each square with the help of a regular grid).
134 A supplementary set of samples used for validation purposes (see paragraph *Model validation*) was
135 collected in 2013 in the early part of the season (June and July) with a different data design: in this
136 case, each sample was cut within a different plot, to improve spatial distribution of points. Points
137 were randomly generated on a 250 × 250 m grid with stratification (5 points in each cell) within
138 alpine grasslands. To grant that validation would not be performed in different environmental
139 conditions from the ones considered during model calibration, point selection was done only within
140 the sectors in which 2012 sampling plots are present, and considering only points included in the
141 altitudinal range of the 2012 dataset (2026-2804 m).
142 Collected samples were weighed (wet weight), dried in a ventilated oven at 60° C for 48 hours and
143 weighed again (dry weight). Samples were analysed as described by Palmonari et al. [2014] to
144 obtain, for each sample, the following nutritional information: (i) the relative content of crude
145 protein (CP), obtained using the official semiautomated method AOAC 976.06 [AOAC, 1990]; (ii)
146 the fraction of neutral detergent fibre (NDF), obtained using the method exposed by Goering and
147 Van Soest [1970] with the modifications of Mertens et al. [2002]; (iii) the fraction of acid detergent
148 fibre (ADF) and lignin (ADL), obtained with the official method AOAC 973.18 [AOAC, 2000]; (iv)
149 the NDF digestibility after 24 hours (dNDF24) and 240 hours (dNDF240), measured by incubating
150 forage in buffer fluids, obtained from rumen fluid of live cows, at body temperature under
151 anaerobic conditions. The dNDF24 is estimated as the fraction of digested NDF after 24 hours,
152 while dNDF240 is estimated from the fraction of indigestible fibre remaining after 240 hours
153 incubation [Goering and Van Soest, 1970].

All the data used in this paper are publicly available on "figshare" repository [Ranghetti and Palmonari, 2015; Ranghetti et al., 2015].

Satellite data

Data taken from the MODIS TERRA MOD09Q1 250 m dataset, validated version V005 [NASA LP DAAC, 2014] were used, selecting all the images relatives to years 2012-2013 for the tile h18v04. This product provides composite images with a period of 8 days (in which the value of each pixel is the best value considering all 8 days) and two spectral bands, RED (red band, 620 – 670 nm) and NIR (near infrared band, 841 – 846 nm). Information about the day of acquisition of each pixel (DOY: Day of the Year, the progressive integer starting from the beginning of the solar year) was taken from the MODIS MOD09A1 product, since the MOD09Q1 dataset does not provide them.

Preprocessing of MODIS images has been done using R [R Core Team, 2014], GDAL 1.11.0 [Warmerdam, 2008] and Modis Reprojection Tool (https://lpdaac.usgs.gov/tools/modis_reprojection_tool). The script used is publicly available as part of the "LR EstGrass" project on GitHub [Ranghetti, 2015].

Images were maintained in the original sinusoidal projection to avoid reshaping noise. NDVI maps were obtained by applying, for each pixel, the formula (NIR – RED) / (NIR + RED).

Nineteen seasonal series from 2012 NDVI maps were considered, extracting values at the plot positions. Since spatial resolution (250 m) is quite coarse in a heterogeneous environment, each pixel value can vary consistently from its neighbours; for this reason, associating to each plot the exact value of the pixel in which the plot lies appeared rough estimated. Therefore, each value was computed from its image with a bidimensional 3×3 kernel gaussian lowpass filter ($\sigma = 1$), taking into account the distance from each plot to the centres of the nearest pixels. To filter unrealistic extreme variability from our data, values identifiable as isolated peaks or pits (NDVI values whose difference from both the preceding and the succeeding value was more than 0.1) were first erased; then the series were smoothed by fitting a local polynomial regression [Cleveland et al., 1992] between NDVI and time. With these methods seasonal series resulted more homogeneous, but they

180 are not continuous, since only one value for each period of eight days is available. To obtain daily
181 values for each time series, the predictions were extended using a spline interpolation [Press et al.,
182 1992].
183 The NDVI values were extracted from this preprocessed daily dataset in order to relate to each field
184 record (using values which refer to the exact days of acquisition of each field sample); time series
185 of experimental plots are shown in Figure 3. This work-frame has been used also for the field data
186 collected in 2013.
187 [Figure 3 about here]

188 ## *Data analysis*

189 ### Dependent variables and predictors

190 Data analysis was performed with the open source statistical environment R version 3.1.1 [R Core
191 Team, 2014] using packages sp [Pebesma and Bivand, 2005], rgdal [Bivand et al., 2014], raster
192 [Hijmans, 2014], relaimpo [Grömping, 2006] and car [Fox and Weisberg, 2011]. The script used is
193 publicly available as part of the "LR EstGrass" project on GitHub [Ranghetti, 2015] (release 1.0).
194 The relationships between predictors and the following nutritional parameters as dependent
195 variables (Y) were modelled: Aboveground biomass (AB), crude protein (CP), neutral detergent
196 fibre (NDF), acid detergent fibre (ADF), lignin (ADL), NDF digestibility at 24 hours (dNDF24) and
197 NDF digestibility at 240 hours (dNDF240). AB is an absolute measure (expressed in grams), while
198 the others are relative measures on total content (range 0-1). Each nutritional parameter was
199 modelled separately as a dependent variable (Y).
200 In order to estimate these nutritional parameters, both morphometric and phenological parameters
201 were used. While morphometric predictors can be easily obtained from a Digital Elevation Model
202 (DEM), phenological parameters depends on seasonality; thus remotely sensed information is
203 necessary to estimate them. Details about the used predictors and the methods to quantify or
204 estimate them are described below.
205 *Elevation*

206 Elevation was extracted from the 10 m TINITALY digital elevation model [Tarquini et al., 2007;
207 Tarquini et al., 2012]. Elevation values have been computed with a 3 × 3 kernel gaussian lowpass
208 filter, as done for the NDVI values.

209 *North-South aspect*

210 An aspect map was derived from the elevation map and values were computed using the nearest
211 neighbour method. From this map the North-South component of the aspect (aspectNS) was derived
212 as the additive inverse of cosine of the aspect, which can vary from –1 (North) to 1 (South).

213 *Beginning of growing season*

214 The date of beginning of the growing season (BGS) represents a temporal metric useful to
215 synthesise the variability between phenology of different stations [Chen et al., 2000]. BGS was
216 estimated as the day when each seasonal series reached a threshold relative value t (a threshold is a
217 fraction of the maximal annual NDVI range). Figure 4 represents how this metric (along with Dmax
218 and NDVImax, described in the following paragraphs) were computed. This approach was proposed
219 by Fontana et al. [2008] who used a value of $t \approx 0.75$ to estimate the BGS. However, this value of t
220 cannot be used with our data because of the different spatial resolution (250 m in our case and
221 500 m in Fontana et al. [2008]). Thus, t was recomputed using NDVI time series compared with our
222 2012 field data, obtaining $t = 0.51$ as best threshold value. The methodology of this estimation is
223 described in supplementary material S1, along with the analysis of the efficiency.

224 [Figure 4 about here]

225 BGS dates were used also to recompute, for each sample, the date from solar progressive Day Of
226 the Year (DOY) to phenological day (DOS, Day Of the Season): DOS = DOY – BGS.

227 *NDVI maximum value*

228 NDVI is a measure of reflectivity, and its relation with biomass is known [Pettorelli et al., 2005;
229 Boschetti et al., 2009]. So the maximum NDVI value (NDVImax) can provide information about
230 the maximum seasonal productivity. This metric was simply computed as the maximum value
231 among all the daily ones within each plot.

Day of NDVI maximum value

The date in which this maximum NDVI value was reached (Dmax) was also considered as a proxy for the day of peak of the season: in fact, the NDVI decrease corresponds to a senescence of vegetation, so the starting day of this decrease may represent the moment in which grass stops to increment its biomass and begins to dry.

Daily NDVI

Daily values of NDVI were used in combination with DOY (Day Of the Year) or DOS (Day Of the season) in order to allow the generation of daily measures of the Y dependent variables (see paragraph *Satellite data* for the preprocessing methods used to obtain daily NDVI values).

Model development

Here are described the models used to estimate Y dependent variables. First, the correlation matrix between predictors was computed in order to avoid collinearity (using Spearman's rank correlation ρ coefficients). Three couple of variables resulted autocorrelated: BGS-Dmax ($\rho = 0.75$, p-value = 0.0011), BGS-elevation ($\rho = 0.90$, p-value $< 10^{-4}$) and Dmax-elevation ($\rho = 0.81$, p-value = 0.0002): for this reason, elevation and Dmax were excluded.

Then, for each dependent variable, the following possible predictive linear models were built (using here and in the rest of the paper the modified Wilkinson-Rogers notation for linear models [Wilkinson and Rogers, 1973], widely used in statistical languages such as R):

1) $Y \sim BGS + NDVImax + aspectNS + NDVI \times DOY$
2) $Y \sim BGS + NDVImax + aspectNS + NDVI \times (DOY + DOY^2)$
3) $Y \sim BGS + NDVImax + aspectNS + NDVI \times (DOS + DOS^2)$

Model selection was performed based on the Akaike Information Criterion [Akaike, 1974; Burnham and Anderson, 2002]. A linear model with DOS (Day Of the Season) at first order only was not built, since DOS is a linear combination of DOY and BGS, so this model would present the same AIC as the first model.

In order to evaluate the relative impact of each predictor, which is fundamental to understand the contribution of each predictor to the estimation of Y dependent variables, the R^2 contribution averaged over orderings among regressors [Lindeman et al., 1980; Chevan and Sutherland, 1991] were computed. The adjusted R^2 (adj-R^2) of the final models were also computed to measure the proportion of predicted variance. Moreover, the R^2 of the univariate models between each response variable and NDVI were computed to better check the proportion of variance which is explained by NDVI oneself.

Model validation

To validate these models two different methods were used: a leave-one-out cross-validation [Picard and Cook, 1984] and a validation with data collected during season 2013.

Since the season 2013 was quite different from the precedent, with a delayed snow melting (about 3 weeks) and summer temperatures generally lower, the use of the 2013 dataset allows to check the robustness and generalisation power of the defined models; also, it allows to improve the spatial interpolation, since the samples were collected in a greater number of plots (114 instead of 19; see paragraph *Field data*).

Validation was performed using RMSE (Root-Mean-Square Error) and MAE (Mean-Average Error).

Normalised values of RMSE and MAE (respectively NRMSE and NMAE) were also computed as the ratio between RMSE or MAE and the ranges of the Y in the 2012 datasets, in order to obtain values which are comparable being on the same scale. The residual distributions (mean and standard error) were also considered to detect the presence of bias in the predictions.

Results and discussion

Seasonal trend of variables

Figure 5 (solid lines) shows the trend of variables during the season.

[Figure 5 about here]

While protein content (CP) and NDF digestibility at 24 hours (dNDF24) present a clear decreasing trend, fibre variables (NDF, ADF and ADL) increase during the season. In particular, crude protein shows a very regular trend into each plot seasonal series: once the day of beginning of growing season (DOS) has been reached, the protein content shows a regular decrease, in agreement with results of other studies [Pérez Corona et al., 1998; Mountousis et al., 2011]. Aboveground biomass (AB) and NDF digestibility at 240 hours (dNDF240) do not show a clear trend (but it is possible to notice an increase of biomass in the first part of the season).

Model characteristics and role of variables

The relative importance of each predictor in the models was summarised in Table 1. It is possible to notice that the predictor with the greater R^2 contribution is time (Day of the Year – DOY – or Day of the Season - DOS – at first and second order); only in the case of aboveground biomass (AB) DOY is not the predictor with the greater R^2 contribution. This evidences are in agreement with the seasonal trend of variables discussed in the paragraph above (the presence of a regular seasonal trend is reflected by a high relative importance of DOY).

[Table 1 about here]

The remaining portion of variance is mainly explained by remote sensing derived predictors: the date of beginning of growing season (BGS), the maximum seasonal NDVI value (NDVImax) and the daily NDVI value (NDVI). It is interesting to notice that daily NDVI solely explains a limited portion of variance (generally between 0.01 and 0.06, and greater than 0.10 only in the case of AB), while the contribution of seasonal parameters derived from NDVI (BGS + NDVImax) is greater (between 0.07 and 0.24). The univariate relation between each experimental variable and NDVI better highlights the lack of direct correlation between these two quantities (see Table 2): indeed, with the exception of AB, for which a correlation with NDVI is shown, although low ($R^2 = 0.25$), in all the other cases R^2 are lower than 0.10. These results show that, in accordance with the literature [Mueller et al., 2008; Pettorelli et al., 2011], NDVI used as a single proxy is a very poor predictor of

307 the nutritional properties of Alpine grasslands, explaining not more than 10% of the total variance
308 in most of the examined nutritional properties of Alpine grasslands.
309 [Table 2 about here]
310 This fact is evident also from Figure 5: the more variance is explained from the temporal predictor,
311 the more the temporal trend of variable is regular. So in the case of biomass, in which the temporal
312 predictor has a lower effect, the predicted values do not present a regular trend, since they are
313 affected by each single NDVI value. At the opposite, when the day of the year has a higher
314 importance there is a clear regular trend. For example, the predictions of CP are driven by a clear
315 second order decreasing trend, that fits well the measured values. Also the predictions of NDF
316 digestibility at 24 hours are linearly decreasing during the season. Predictions of neutral detergent
317 and acid detergent fibre are instead linearly increasing. Globally, adjusted R^2 values ≈ 0.5 were
318 found for most of the models, with the exception of crude protein (adj-$R^2 = 0.8$) and of NDF
319 digestibility at 240 hours (adj-$R^2 = 0.33$): these values demonstrate that models fit quite well field
320 data, in consideration of the high environmental heterogeneity of the study area.

321 ***Model validation***

322 The use of both cross-validation and validation on an independent dataset allowed to analyse the
323 robustness of each model to temporal extrapolation.
324 [Table 3 about here]
325 [Figure 6 about here]
326 Table 3 shows validation metrics computed on both 2012 and 2013 validation sets, while Figure 6
327 compared measured and predicted values for 2012 and 2013. Using the 2012 dataset allows to
328 obtain results that confirmed the calibration metrics (RMSE are generally acceptable, with NRMSE
329 values never greater than 0.20, and mean Y differences are close to zero).
330 The model validation using the 2013 dataset led to different results. With the exception of biomass
331 (AB), which showed results comparable with 2012 cross-validation ones, RMSE and MAE values
332 result greater than with the 2012 data, providing thus less support to the models. Validation with the

2013 dataset provided worse results, which in some cases allowed to recognise the predictive power of models (CP, NDF and dNDF24), while in some others forced to reject them (ADF, ADL and dNDF240). Results about each single variable are discussed below.

Aboveground biomass. The only variable for which 2013 validation metrics are better than 2012 ones is biomass (AB). This model is well supported by the results of the validation model (NRMSE = 0.11 and NMAE = 0.09, values which are acceptable and lower than in 2012) and its predictions are not biased ($\Delta Y = -4 \pm 16$ g). The reason of that could be attributed to the low portion of variance explained by temporal predictor (DOY and DOY^2): thanks to this, it was possible to better make temporal extrapolations.

Crude protein. The predictive power of crude protein (CP) decreased using 2013 dataset (NRMSE = 0.14 and NMAE = 0.11, while with cross-validation these values are respectively 0.09 and 0.07), but these values are comparable with the values obtained for other well-predicted variables, and predictions are not biased ($\Delta Y = 0.00 \pm 0.03$ g): for this reason, CP can still be considered predictable.

Fibre digestibility. Regarding the digestibility, is it possible to notice a different behaviour between NDF digestibility at 24 (dNDF24) and 240 hours (dNDF240). In the first case models are able to explain about half of the total variance, and validation metrics for 2013 dataset (NRMSE = 0.16, MAE = 0.13) are not different from the ones in 2012 (NRMSE = 0.14, NMAE = 0.11); however a little bias in the 2013 predictions is present ($\Delta Y = -0.07 \pm 0.05$; see also a graphical overestimations in Figure 6). The reason of this bias could be similar to the one hypothesised for crude protein: since the temporal predictors are more important in the model than NDVI, predicting values in a different season could produce less accurate results. NDF digestibility at 240 hours cannot be predicted, since its model explains too little variance (adj-R^2 = 0.329).

Fibre. Also in the predictions for fibres a difference similar as in the case of digestibility was noticed. In the case of neutral detergent fibre (NDF) the model is quite good and supported by validation results (NRMSE = 0.16, NMAE = 0.14 for 2013); a bias is not evident from ΔY

359 distribution ($\Delta Y = 0.03 \pm 0.06$), but a little underestimation is graphically suggested. Acid detergent
360 fibre (ADF) and lignin (ADL) models have to be rejected because validation with 2013 data clearly
361 fails (NRMSE = 0.4, NMAE = 0.4 for ADF; NRMSE = 0.5, NMAE = 0.4 for ADL). There is a
362 possible reason for these difference within both fibre and digestibility (predictability of dNDF24
363 and NDF but not of dNDF240, ADF and ADL) considering the nature of these variables: cellulose
364 and lignin are the vegetal component which less manifest themselves into visible effects (like
365 greenness), and NDF digestibility at 240 hours is linked to their relative content more than in the
366 case of NDF digestibility at 24 hours [Clipes et al., 2006; Casali et al., 2008].

367 ***Models' improvement***

368 All these results evidence how remotely sensed information can contribute to predict the daily
369 values of nutritional content of grassland, since the relative importance of remote sensing derived
370 predictors (measured as R^2 relative contribution) is quite relevant. Nevertheless, the experimental
371 design used for this work did not allow to take advantage of inter-annual variability for the
372 calibration of models, since they are built basing on field data collected in a single growing season;
373 consequently, temporal extrapolation made on 2013 dataset (which cannot be used also for
374 calibration, since samples are not collected during the whole growing season) evidenced a loss in
375 predictive performance. For these reasons, a recalibration of models performed on a field dataset
376 collected on a longer time window appear to be convenient before an operational use of models.
377 Furthermore, the use of different vegetation indices could also be exploited [Barati et al., 2011].
378 However, in this paper only NDVI was considered because additional MODIS spectral bands,
379 required for the computation of most of these indices (typically blue or green bands), are not
380 available at 250 m resolution. Making a spatial disaggregation of these bands or using data at 500 m
381 or 1 km spatial resolution was avoided, since it could be potentially misleading in the context of
382 high environmental heterogeneity of our study area. Equally, the use of different remotely sensed
383 data (multi-spectral or hyper-spectral) appeared inconsistent with the perspective of an analysis of
384 the vegetation dynamics in the past, since a temporal resolution of few days is required in the

385 context of our study area (in which cloud cover is frequent), and in our knowledge no other data
386 sets with a sufficiently good temporal resolution are freely available for the past fifteen years.

387 Conclusions

388 This study showed how satellite data can be useful to estimate some important bromatological
389 properties of alpine grasslands.
390 First, the correlation between single NDVI values and nutritional variables resulted low (in the case
391 of biomass, a variable for which a direct link with the vegetation index is known) or absent (in the
392 other cases): this result evidenced how the use of this remotely sensed index as a proxy for them can
393 lead to errors. Nevertheless, MODIS data resulted useful for the estimation of temporal dynamics of
394 pastures, which concur to explain a substantial portion of variance in terms of R^2 contribution. In
395 particular, dates of beginning of growing season (BGS) predicted from satellite data showed a high
396 correlation with ground truth (adj-R^2 = 0.84), confirming the validity of our method.
397 The possibility to estimate phenological predictors from MODIS data allowed to make predictive
398 models of nutritional variables; anyway, it is evident that not all these variables can be predicted in
399 the same way and with the same accuracy. Our results showed that the defined models allow to
400 make predictions on biomass, crude protein, NDF digestibility at 24 hours and neutral detergent
401 fibre, but not on NDF digestibility at 240 hours, acid detergent fibre and lignin. In the case of
402 biomass, protein and neutral detergent fibre (and partially with NDF digestibility at 24 hours) the
403 goodness of these models for doing temporal extrapolations was confirmed by validating them with
404 2013 data.
405 Our findings pave the road for a multi-annual analysis of changes in nutritional content of Alpine
406 grasslands in terms of crude protein, NDF digestibility at 24 hours, neutral detergent fibre and
407 biomass, which could be potentially useful to better understand the complex effects of climate
408 change on the population dynamics of Alpine herbivores. However, in order to predict variable
409 depending on specific seasonal condition with empirical multivariate model it is convenient to have
410 a calibration dataset that includes multi annual data; so, to improve temporal robustness the

411 recalibration of the models with field data collected in other seasons appears convenient before
412 operationally use them.

413 Acknowledgments

414 This study has been funded by EU InterReg project "GREAT" (*Grandi Erbivori negli Ecosistemi*
415 *Alpini in Trasformazione*, http://www.greatinterreg.eu), a joint project by the Gran Paradiso
416 National Park and the Swiss National Park. We thank Domenico Bergero for his help with the
417 bromatological analysis on field samples, and Mirco Boschetti for the helpful advices, which
418 concurred to improve the quality and clarity of work. We are grateful to the many people who
419 helped us in various ways with field work: Natalia Santoro, Alice Brambilla, Caterina Ferrari,
420 Alberto Peracino, Raffaella Miravalle, Ramona Viterbi, Emanuel Rocchia, Marco Solive, Piero
421 Troja, Martina Silba, Xavier Bal, Federica Pellicioli, Sara Bernardini and Walter Giannoccaro. We
422 also thank the park wardens of Gran Paradiso National Park for their logistic support. Finally, we
423 are grateful to the NASA/MODIS Land Discipline Group for producing and sharing MODIS
424 datasets.

425 References

426 Akaike, H. (1974). *A New Look at the Statistical Model Identification*. IEEE Transactions on
427 Automatic Control, AC-19, 6, pp. 716–723. doi: http://dx.doi.org/10.1109/TAC.1974.1100705.
428 AOAC (1990). *Protein (crude) in animal feed (976.06)*. Official Methods of Analysis of the
429 Association of Official Analytical Chemists. 15th Ed., p. 72.
430 AOAC (2000). *Fiber (Acid Detergent) and Lignin in Animal Feed (973.18)*. Official Methods of
431 Analysis of the Association of Official Analytical Chemists. 17th Ed., p. 72.
432 Barati S., Rayegani B., Saati M., Sharifi A., Nasri M. (2011). *Comparison the accuracies of*
433 *different spectral indices for estimation of vegetation cover fraction in sparse vegetated areas*.
434 Egyptian Journal of Remote Sensing and Space Science, 14, 1, pp. 49–56. doi:
435 http://dx.doi.org/10.1016/j.ejrs.2011.06.001.

436 Beeri O., Phillips R., Hendrickson J., Frank A.B., Kronberg S. (2007). *Estimating forage quantity*
437 *and quality using aerial hyperspectral imagery for northern mixed-grass prairie*. Remote
438 Sensing of Environment, 110, 2, pp. 216–225. doi: http://dx.doi.org/10.1016/j.rse.2007.02.027.
439 Bivand R., Keitt T., Rowlingson B. (2014). *rgdal: Bindings for the Geospatial Data Abstraction*
440 *Library*. http://CRAN.R-project.org/package=rgdal.
441 Boone R.B., Thirgood S., Hopcraft J. (2006). *Serengeti wildebeest migratory patterns modeled from*
442 *rainfall and new vegetation growth*. Ecology, 87, 8, pp. 1987–1994.
443 Boschetti M., Bocchi S., Brivio P.A. (2007). *Assessment of pasture production in the Italian Alps*
444 *using spectrometric and remote sensing information.* Agriculture, Ecosystems & Environment,
445 118, pp. 267-272. doi: http://dx.doi.org/10.1016/j.agee.2006.05.024.
446 Boschetti M., Stroppiana D., Brivio P.A., Bocchi S. (2009). *Multi-year monitoring of rice crop*
447 *phenology through time series analysis of MODIS images.* International Journal of Remote
448 Sensing, 30, pp. 4643-4662. doi: http://dx.doi.org/10.1080/01431160802632249.
449 Burnham K.P., Anderson D.R. (2002). *Model selection and multimodel inference: a practical*
450 *information-theoretic approach*. Springer Science & Business Media. doi:
451 http://dx.doi.org/10.1007/b97636.
452 Casali A., Detmann E., Valadares Filho S., Pereira J., Henriques L., De Freitas S., Paulino M.
453 (2008). *Influência do tempo de incubacão e do tamanho de partículas sobre os teores de*
454 *compostos indigestíveis em alimentos e fezes bovinas obtidos por procedimentos in situ*. Revista
455 Brasileira de Zootecnia, 37, 2, pp. 335–342.
456 Casanova D., Epema G., Goudriaan J. (1998), *Monitoring rice reflectance at field level for*
457 *estimating biomass and LAI*. Field Crops Research, 55, 1-2, pp. 83–92. doi:
458 http://dx.doi.org/10.1016/S0378-4290(97)00064-6.
459 Chen X., Tan Z., Schwartz M., Xu C. (2000). *Determining the growing season of land vegetation*
460 *on the basis of plant phenology and satellite data in Northern China*. International Journal of
461 Biometeorology, 44, 2, pp. 97–101.

462 Chevan A., Sutherland M. (1991). *Hierarchical Partitioning*. The American Statistician 45, pp. 90–
463 96.
464 Cleveland W.S., Grosse E., Shyu W.M. (1992). *Local regression models*, in *Statistical Models in S*,
465 ed. by J. M. Chambers and T. J. Hastie, Taylor Francis, chap. 8.
466 Clipes R., Detmann E., Silva J., Vieira R., Nunes L., Lista F., Ponciano N. (2006), *Evaluation of*
467 *acid detergent insoluble protein as an estimator of rumen non-degradable protein in tropical*
468 *grass forages*. Arquivo Brasileiro de Medicina Veterinaria e Zootecnia, 58, 4, pp. 694–697.
469 Cong N., Wang T., Nan H., Ma Y., Wang X., Myneni R., Piao S. (2013). *Changes in satellite-*
470 *derived spring vegetation green-up date and its linkage to climate in China from 1982 to 2010:*
471 *A multimethod analysis*. Global Change Biology, 19, 3, pp. 881–891. doi:
472 http://dx.doi.org/10.1111/gcb.12077.
473 Cordova F., Wallace J.D., Pieper R.D. (1978). *Forage intake by grazing livestock: a review*. Journal
474 of Range Management, pp. 430–438. doi: http://dx.doi.org/10.2307/3897201.
475 Darvishzadeh R., Skidmore A., Schlerf M., Atzberger C., Corsi F., Cho M. (2008), *LAI and*
476 *chlorophyll estimation for a heterogeneous grassland using hyperspectral measurements*.
477 ISPRS Journal of Photogrammetry and Remote Sensing, 63, 4, pp. 409–426. doi:
478 http://dx.doi.org/10.1016/j.isprsjprs.2008.01.001.
479 Di Bella C. , Paruelo J., Becerra J., Bacour C., Baret F. (2004). *Effect of senescent leaves on NDVI-*
480 *based estimates of fAPAR: Experimental and modelling evidences*. International Journal of
481 Remote Sensing, 25, 23, pp. 5415–5427. doi: http://dx.doi.org/10.1080/01431160412331269724.
482 Elvidge C., Lyon R. (1985), *Influence of rock-soil spectral variation on the assessment of green*
483 *biomass*. Remote Sensing of Environment, 17, 3, pp. 265–279. doi:
484 http://dx.doi.org/10.1016/0034-4257(85)90099-9.
485 Fensholt R., Sandholt I., Rasmussen M. (2004). *Evaluation of MODIS LAI, fAPAR and the relation*
486 *between fAPAR and NDVI in a semi-arid environment using in situ measurements*. Remote
487 Sensing of Environment, 91, 3-4, pp. 490–507. doi: http://dx.doi.org/10.1016/j.rse.2009.04.004.

Fontana F., Rixen C., Jonas T., Aberegg G., Wunderle S. (2008), *Alpine grassland phenology as seen in AVHRR, VEGETATION, and MODIS NDVI time series - A comparison with in situ measurements*. Sensors, 8, 4, pp. 2833–2853. doi: http://dx.doi.org/10.3390/s8042833.

Fox J., Weisberg S. (2011). *An R Companion to Applied Regression*. Second, Sage, Thousand Oaks CA.

Gao Q., Li Y., Wan Y., Qin X., Jiangcun W., Liu Y. (2009). *Dynamics of alpine grassland NPP and its response to climate change in Northern Tibet*. Climatic Change, 97, 3, pp. 515–528. doi: http://dx.doi.org/10.1007/s10584-009-9617-z.

Gitelson A., Peng Y., Huemmrich K. (2014). *Relationship between fraction of radiation absorbed by photosynthesizing maize and soybean canopies and NDVI from remotely sensed data taken at close range and from MODIS 250m resolution data*. Remote Sensing of Environment, 147, pp. 108–120. doi: http://dx.doi.org/10.1016/j.rse.2014.02.014.

Gnyp M., Miao Y., Yuan F., Ustin S., Yu K., Yao Y., Huang S., Bareth G. (2014), *Hyperspectral canopy sensing of paddy rice aboveground biomass at different growth stages*. Field Crops Research, 155, pp. 42–55. doi: http://dx.doi.org/10.1016/j.fcr.2013.09.023.

Goering H., Van Soest P. (1970). *Forage Fiber Analysis. USDA Agricultural Research Service. Handbook number 379*. US Department of Agriculture. Superintendent of Documents, US Government Printing Office, Washington, DC.

González-Alonso F., Merino-De-Miguel S., Roldán-Zamarrón A., García-Gigorro S., Cuevas J. (2006). *Forest biomass estimation through NDVI composites. The role of remotely sensed data to assess Spanish forests as carbon sinks*. International Journal of Remote Sensing, 27, 24, pp. 5409–5415. doi: http://dx.doi.org/10.1080/01431160600830748.

Griffith B., Douglas D., Walsh N., Young D., McCabe T., Russell D., White R., Cameron R., Whitten K. (2002). *The Porcupine caribou herd*, in *Arctic Refuge coastal plain terrestrial wildlife research summaries*, ed. by D. C. Douglas, P. E. Reynolds and E. B. Rhode, U. S. Geological Survey, Biological Resources Division, chap. 3, pp. 8–37.

514 Grömping U (2006). *Relative Importance for Linear Regression in R: The Package relaimpo.*
515 Journal of Statistical Software, 17, 1, pp. 1–27.
516 Hamel S., Garel M., Festa-Bianchet M., Gaillard J.-M., Côté S.D. (2009). *Spring Normalized*
517 *Difference Vegetation Index (NDVI) predicts annual variation in timing of peak faecal crude*
518 *protein in mountain ungulates*. Journal of Applied Ecology, 46, 3, pp. 582–589. doi:
519 http://dx.doi.org/10.1111/j.1365-2664.2009.01643.x.
520 Hijmans R.J. (2014). *raster: Geographic data analysis and modeling*. http://R-Forge.R-
521 project.org/projects/raster/.
522 Hodgman T., Davitt B., Nelson J. (1996). *Monitoring mule deer diet quality and intake with fecal*
523 *indices*. Journal of Range Management, 49, 3, pp. 215–222.
524 Huete A., Jackson R., Post D. (1985). *Spectral response of a plant canopy with different soil*
525 *backgrounds*. Remote Sensing of Environment, 17, 1, pp. 37–53. doi:
526 http://dx.doi.org/10.1016/0034-4257(85)90111-7.
527 Huete A., Tucker C. (1991). *Investigation of soil influences in AVHRR red and near-infrared*
528 *vegetation index imagery*. International Journal of Remote Sensing, 12, 6, pp. 1223–1242. doi:
529 http://dx.doi.org/10.1080/01431169108929723.
530 Islam M., Garcia S., Henry D. (2011). *Use of normalised difference vegetation index, nitrogen*
531 *concentration, and total nitrogen content of whole maize plant and plant fractions to estimate*
532 *yield and nutritive value of hybrid forage maize*. Crop and Pasture Science, 62, 5, pp. 374–382.
533 doi: http://dx.doi.org/10.1071/CP10244.
534 Jacobson A., Provenzale A., von Hardenberg A., Bassano B., Festa-Bianchet M. (2004), *Climate*
535 *forcing and density dependence in a mountain ungulate population*. Ecology, 85, 6, pp. 1598–
536 1610.
537 Leslie D., Starkey E. (1985) *Fecal indices to dietary quality of cervids in old-growth forests*.
538 Journal of Wildlife Management, 49, 1, pp. 142–146.

539 Li G., Wang D., Liu S., Fan W., Zhang H., Xin X., Zhang H. (2010). *Validation of MODIS FAPAR*
540 *products in hulunber grassland of China*, in *Geoscience and Remote Sensing Symposium*
541 *(IGARSS)*, IEEE, Honolulu, HI, pp. 1047–1050. doi:
542 http://dx.doi.org/10.1109/IGARSS.2010.5650113.
543 Liang S., Peng S., Lin X., Cong N. (2013). *NDVI-based spatial-temporal change in grassland*
544 *growth of China from 1982 to 2010*. Beijing Daxue Xuebao (Ziran Kexue Ban)/Acta
545 Scientiarum Naturalium Universitatis Pekinensis, 49, 2, pp. 311–320.
546 Lindeman R.H., Merenda P.F,. Gold R.Z. (1980). *Introduction to Bivariate and Multivariate*
547 *Analysis*. Glenview IL: Scott, Foresman.
548 Madugundu R., Nizalapur V., Jha C. (2008). *Estimation of LAI and above-ground biomass in*
549 *deciduous forests: Western Ghats of Karnataka, India*. International Journal of Applied Earth
550 Observation and Geoinformation, 10, 2, pp. 211–219. doi:
551 http://dx.doi.org/10.1016/j.jag.2007.11.004.
552 Mao D.-H., Wang Z.-M., Luo L., Han J.-X. (2012). *Dynamic changes of vegetation net primary*
553 *productivity in permafrost zone of Northeast China in 1982-2009 in response to global change*.
554 Chinese Journal of Applied Ecology, 23, 6, pp. 1511–1519.
555 Marti J., Bort J., Slafer G., Araus J. (2007). *Can wheat yield be assessed by early measurements of*
556 *Normalized Difference Vegetation Index?*. Annals of Applied Biology, 150, 2, pp. 253–257. doi:
557 http://dx.doi.org/10.1111/j.1744-7348.2007.00126.x.
558 Mertens D., Allen M., Carmany J., Clegg J., Davidowicz A., Drouches M., Frank K., Gambin D.,
559 Garkie M., Gildemeister B., Jeffress D., Jeon C.-S., Jones D., Kaplan D., Kim G.-N., Kobata S.,
560 Main D., Moua X., Paul B., Robertson J., Taysom D., Thiex N., Williams J., Wolf M. (2002),
561 *Gravimetric determination of amylase-treated neutral detergent fiber in feeds with refluxing in*
562 *beakers or crucibles: Collaborative study*. Journal of AOAC International, 85, 6, pp. 1217–1240.

563 Mignatti A., Casagrandi R., Provenzale A., von Hardenberg A., Gatto M. (2012). *Sex- and age-*
564 *structured models for Alpine ibex Capra ibex ibex population dynamics*. Wildlife Biology, 18, 3,
565 pp. 318–332. doi: http://dx.doi.org/10.2981/11-084.
566 Moreau S., Bosseno R., Gu X., Baret F. (2003). *Assessing the biomass dynamics of Andean bofedal*
567 *and totora high-protein wetland grasses from NOAA/AVHRR*. Remote Sensing of Environment,
568 85, 4, pp. 516–529. doi: http://dx.doi.org/10.1016/S0034-4257(03)00053-1.
569 Mountousis I., Dotas V., Stanogias G., Papanikolaou K., Roukos C., Liamadis D. (2011).
570 *Altitudinal and seasonal variation in herbage composition and energy and protein content of*
571 *grasslands on Mt Varnoudas, NW Greece*. Animal Feed Science and Technology, 164, 3-4, pp.
572 174–183. doi: http://dx.doi.org/10.1016/j.anifeedsci.2011.01.007.
573 Mueller T., Olson K., Fuller T., Schaller G., Murray M., Leimgruber P. (2008). *In search of forage:*
574 *Predicting dynamic habitats of Mongolian gazelles using satellite-based estimates of vegetation*
575 *productivity*. Journal of Applied Ecology, 45, 2, pp. 649–658. doi:
576 http://dx.doi.org/10.1111/j.1365-2664.2007.01371.x.
577 Myneni R., Williams D. (1994). *On the relationship between FAPAR and NDVI*. Remote Sensing of
578 Environment, 49, 3, pp. 200–211. doi: http://dx.doi.org/10.1016/0034-4257(94)90016-7.
579 NASA LP DAAC (2014). *MOD09Q1*. USGS/Earth Resources Observation and Science (EROS)
580 Center, Sioux Falls, South Dakota,
581 https://lpdaac.usgs.gov/products/modis_products_table/mod09q1.
582 Palmonari A., Fustini M., Canestrari G., Grilli E., Formigoni A. (2014). *Influence of maturity on*
583 *alfalfa hay nutritional fractions and indigestible fiber content*. Journal of Dairy Science, 97, 12,
584 pp. 7729–7734. doi: http://dx.doi.org/10.3168/jds.2014-8123.
585 Pebesma E.J., Bivand R. (2005). *Classes and methods for spatial data in R*. R News, 5, 2 (Nov.
586 2005), pp. 9–13.

587 Pérez Corona M., Vâzquez De Aldana B., Criado B., Ciudad A. (1998). *Variations in nutritional*
588 *quality and biomass production of semiarid grasslands*. Journal of Range Management, 51, 5,
589 pp. 570–576.
590 Pettorelli N., Pelletier F., von Hardenberg A., Festa-Bianchet M., Côté S.D. (2007). *Early onset of*
591 *vegetation growth vs. rapid green-up: Impacts on juvenile mountain ungulates*. Ecology, 88, 2,
592 pp. 381–390. doi: http://dx.doi.org/10.1890/06-0875.
593 Pettorelli N., Ryan S., Mueller T., Bunnefeld N., Jedrzejewska B., Lima M., Kausrud K. (2011).
594 *The Normalized Difference Vegetation Index (NDVI): Unforeseen successes in animal ecology*.
595 Climate Research, 46, 1, pp. 15–27. doi: http://dx.doi.org/10.3354/cr00936.
596 Pettorelli N., Vik J., Mysterud A., Gaillard J.-M., Tucker C., Stenseth N. (2005). *Using the satellite-*
597 *derived NDVI to assess ecological responses to environmental change*. Trends in Ecology and
598 Evolution, 20, 9, pp. 503–510. doi: http://dx.doi.org/10.1016/j.tree.2005.05.011.
599 Picard R.R., Cook R.D. (1984). *Cross-Validation of Regression Models*. Journal of the American
600 Statistical Association, 79, 387.
601 Press W.H., Teukolsky S.A., Vetterling W.T., Flannery B.P. (1992). *Numerical Recipes in C: The*
602 *Art of Scientific Computing*, 2nd ed.. Cambridge University Press, New York, NY, USA.
603 Quarmby N., Milnes M., Hindle T., Silleos N. (1993). *Use of multi-temporal NDVI measurements*
604 *from AVHRR data for crop yield estimation and prediction*. International Journal of Remote
605 Sensing, 14, 2, pp. 199–210.
606 R Core Team (2014). *R: A Language and Environment for Statistical Computing*. R Foundation for
607 Statistical Computing, Vienna, Austria, http://www.R-project.org.
608 Ranghetti L. (2015). *Estimation of nutritional properties of alpine grassland from MODIS NDVI*
609 *data: R code*. GitHub project on figshare repository. doi:
610 http://dx.doi.org/10.6084/m9.figshare.1381836.

611 Ranghetti L., Palmonari A. (2015). *Nutritional content of alpine grassland in Gran Paradiso*
612 *National Park, 2013 dataset*. figshare repository. doi:
613 http://dx.doi.org/10.6084/m9.figshare.1375306.
614 Ranghetti L., Stendardi L., Palmonari A. (2015). *Nutritional content of alpine grassland in Gran*
615 *Paradiso National Park, 2012 dataset*. figshare repository. doi:
616 http://dx.doi.org/10.6084/m9.figshare.1375305.
617 Richardson A., Jenkins J., Braswell B., Hollinger D., Ollinger S., Smith M.-L. (2007). *Use of*
618 *digital webcam images to track spring green-up in a deciduous broadleaf forest*. Oecologia, 152,
619 2, pp. 323–334. doi: http://dx.doi.org/10.1007/s00442-006-0657-z.
620 Roberts G. (2001). *A review of the application of BRDF models to infer land cover parameters at*
621 *regional and global scales*. Progress in Physical Geography, 25, 4, pp. 483–511. doi:
622 http://dx.doi.org/10.1191/030913301701543154.
623 Rouse, J.W., R.H. Haas, J.A. Schell, and D.W. Deering (1973). *Monitoring Vegetation Systems in*
624 *the Great Plains with ERTS*, 309-317. Third ERTS Symposium, NASA SP-351 I.
625 Ryan S., Cross P., Winnie J., Hay C., Bowers J., Getz W. (2012). *The utility of normalized*
626 *difference vegetation index for predicting African buffalo forage quality*. Journal of Wildlife
627 Management, 76, 7, pp. 1499–1508. doi: http://dx.doi.org/10.1002/jwmg.407.
628 Sellers P., Berry J., Collatz G., Field C., Hall F. (1992). *Canopy reflectance, photosynthesis, and*
629 *transpiration. III. A reanalysis using improved leaf models and a new canopy integration*
630 *scheme*. Remote Sensing of Environment, 42, 3, pp. 187–216. doi: http://10.1016/0034-
631 4257(92)90102-P.
632 Tan K., Piao S., Peng C., Fang J. (2007). *Satellite-based estimation of biomass carbon stocks for*
633 *northeast China's forests between 1982 and 1999*. Forest Ecology and Management, 240, 1-3,
634 pp. 114–121. doi: http://dx.doi.org/10.1016/j.foreco.2006.12.018.

635 Tarquini S., Isola I., Favalli M., Mazzarini F., Bisson M., Pareschi M., Boschi E. (2007).
636 *TINITALY/01: A new Triangular Irregular Network of Italy*. Annals of Geophysics, 50, 3, pp.
637 407–425.
638 Tarquini S., Vinci S., Favalli M., Doumaz F., Fornaciai A., Nannipieri L. (2012). *Release of a 10-*
639 *m-resolution DEM for the Italian territory: Comparison with global-coverage DEMs and*
640 *anaglyph-mode exploration via the web*. Computers and Geosciences, 38, 1, pp. 168–170. doi:
641 http://dx.doi.org/10.1016/j.cageo.2011.04.018.
642 Thenkabail P., Smith R., De Pauw E. (2000). *Hyperspectral vegetation indices and their*
643 *relationships with agricultural crop characteristics*. Remote Sensing of Environment, 71, 2, pp.
644 158–182. doi: http://dx.doi.org/10.1016/S0034-4257(99)00067-X.
645 Viña A., Gitelson A. (2005). *New developments in the remote estimation of the fraction of absorbed*
646 *photosynthetically active radiation in crops*. Geophysical Research Letters, 32, 17, pp. 1–4. doi:
647 http://dx.doi.org/10.1029/2005GL023647.
648 von Hardenberg A., Bassano B., Peracino V., von Hardenberg J., Provenzale A. (2000). *Preliminary results*
649 *on the temporal variability of the Alpine ibex population in the Gran Paradiso National Park*. Journal of
650 Mountain Ecology, 5, pp. 201-210.
651 Wang F.-M., Huang J.-F., Tang Y.-L., Wang X.-Z. (2007). *Estimation of rice LAI by using NDVI at*
652 *different spectral bandwidths*. Chinese Journal of Applied Ecology, 18, 11, pp. 2444–2450.
653 Wang J., Rich P., Price K., Dean Kettle W. (2005). *Relations between NDVI, grassland production,*
654 *and crop yield in the central great plains*. Geocarto International, 20, 3, pp. 5–11. doi:
655 http://dx.doi.org/10.1080/10106040508542350.
656 Warmerdam F. (2008). *The Geospatial Data Abstraction Library*, in *Open Source Approaches in*
657 *Spatial Data Handling*, ed. by G. Brent Hall and M. G. Leahy, Springer Berlin Heidelberg, pp.
658 87–104.
659 Wilkinson G., Rogers C. (1973), *Symbolic description of factorial models for analysis of variance*.
660 Journal of Applied Statistics, 22, 3, pp. 392–399.

661 Willmott C., Matsuura K. (2005). *Advantages of the mean absolute error (MAE) over the root mean*
662 *square error (RMSE) in assessing average model performance*. Climate Research, 30, 1, pp.
663 79–82.
664 Xu W., Xin Y., Zhang J., Xiao R., Wang X. (2014). *Phenological variation of alpine grasses*
665 *(Gramineae) in the northeastern Qinghai-Tibetan plateau, China during the last 20 years*.
666 Shengtai Xuebao/ Acta Ecologica Sinica, 34, 7, pp. 1781–1793. doi:
667 http://dx.doi.org/10.5846/stxb201303270531.
668 Zha Y., Gao J., Zhang Y. (2005). *Grassland productivity in an alpine environment in response to*
669 *climate change*. Area, 37, 3, pp. 332–340. doi: http://dx.doi.org/10.1111/j.1475-
670 4762.2005.00637.x.
671 Zhang G., Xu X., Zhou C., Zhang H., Ouyang H. (2011). *Responses of grassland vegetation to*
672 *climatic variations on different temporal scales in Hulun Buir Grassland in the past 30 years*.
673 Journal of Geographical Sciences, 21, 4, pp. 634–650. doi: http://dx.doi.org/10.1007/s11442-
674 011-0869-y.
675 Zhang G., Zhang Y., Dong J., Xiao X. (2013). *Green-up dates in the Tibetan Plateau have*
676 *continuously advanced from 1982 to 2011*. Proceedings of the National Academy of Sciences of
677 the United States of America, 110, 11, pp. 4309–4314. doi:
678 http://dx.doi.org/10.1073/pnas.1210423110.

Figures and tables

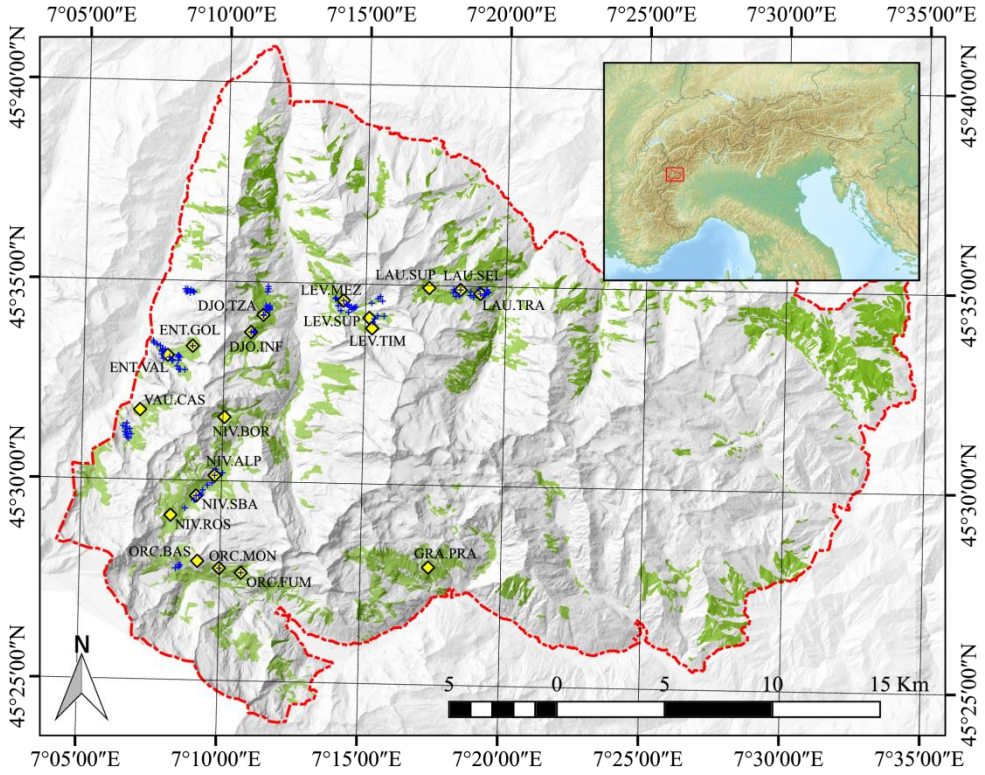

Figure 1 – Position of the 2012 (yellow squares) and 2013 (blue crosses) experimental plots within the Gran Paradiso National Park: red line represents park boundary; green area represents grassland surface; coordinates of the grid are in geographical units (WGS84). Little map shows the position of the Gran Paradiso National Park within the Alps (Background by Lencer via Wikimedia Commons, licence CC BY-SA 3.0).


ORC.FUM, 2012-05-12


ORC.FUM, 2012-06-17


ORC.FUM, 2012-08-11


ORC.FUM, 2012-09-17


NIV.BOR, 2012-06-30


NIV.BOR, 2012-07-15


NIV.BOR, 2012-07-29


NIV.BOR, 2012-09-18

Figure 2 – Photos of two experimental plots, Alpe Fumetta (ORC.FUM, 2145 m) and Plan Borgnoz (NIV.BOR, 2688 m), in four different seasonal growing stages.

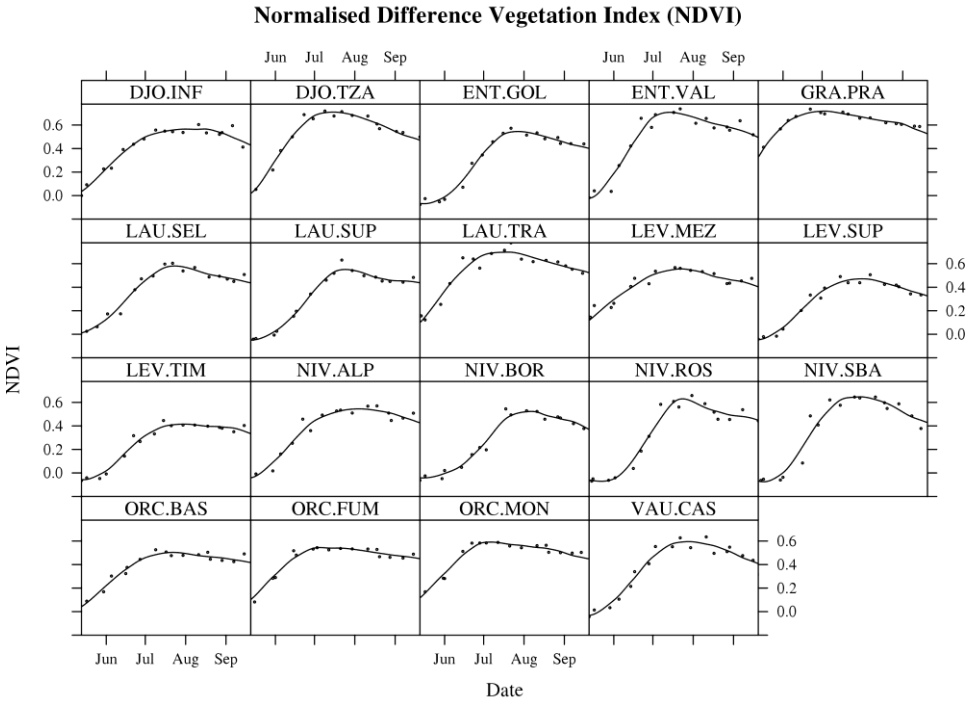

691

692 **Figure 3 – Seasonal trend (2012) of NDVI values. Points are NDVI values computed from MOD09Q1 before the smoothing**
693 **(see paragraph *Satellite data*), lines represent daily smoothed values.**

694

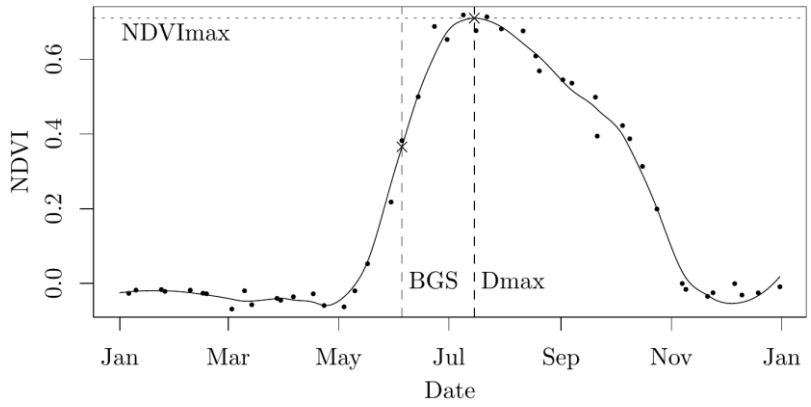

695

696 **Figure 4 – Yearly 2012 NDVI profile of a sampling field plot (DJO.TZA): points are the values taken from MOD09Q1**
697 **products as described in section "Satellite data", line is the daily interpolation. Points marked with "×" are the NDVI values**
698 **corresponding respectively with BGS (51% of the maximum NDVI range) and Dmax (maximum NDVI value: NDVImax).**

699

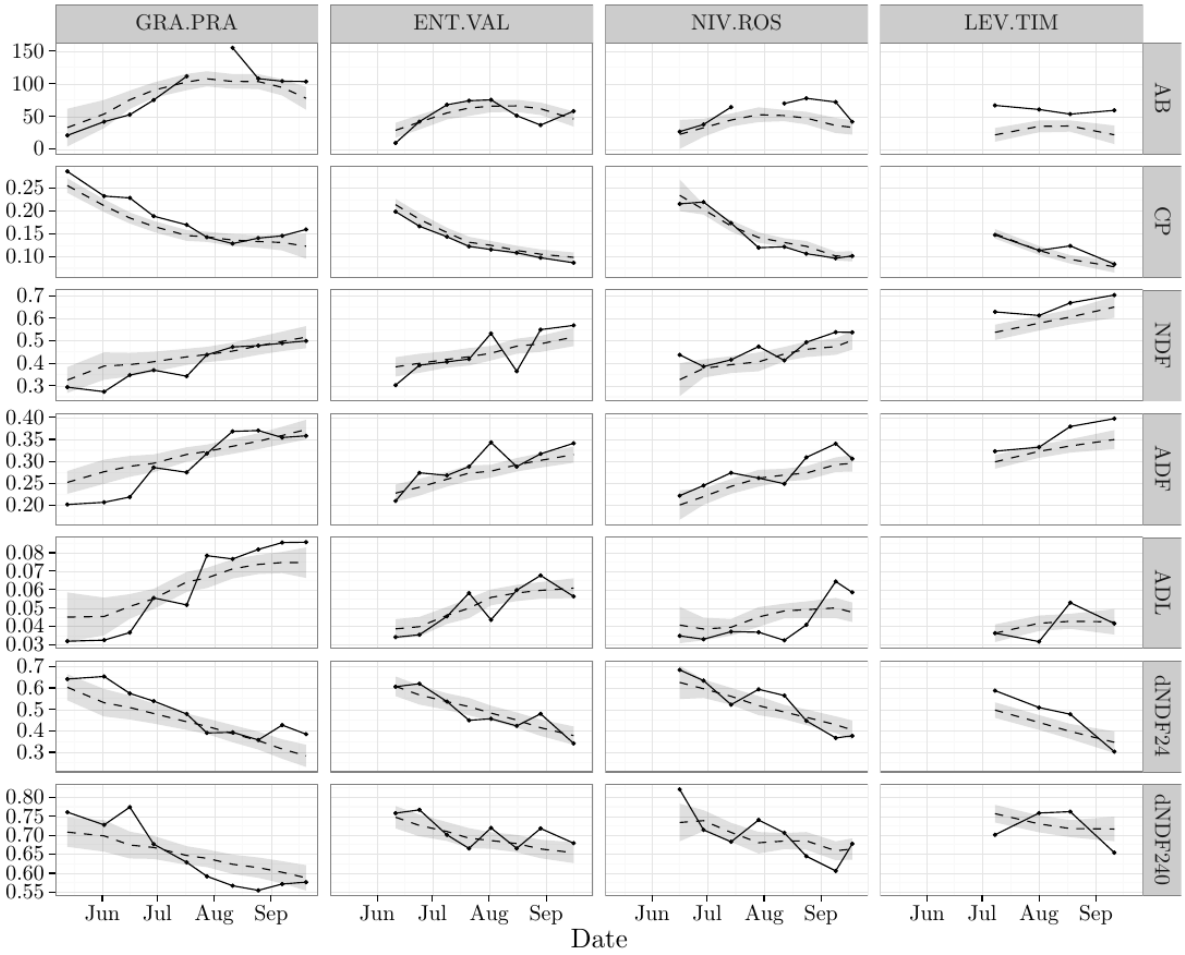

Figure 5 – Seasonal trends (2012) of field variables (each row represents one variable) for 4 sample field sites (one per column; see supplementary material S2 for the graphics of all the 19 field plots). Solid lines represent the field measures, dashed lines represent predicted values, dotted lines border 95% confidence intervals.

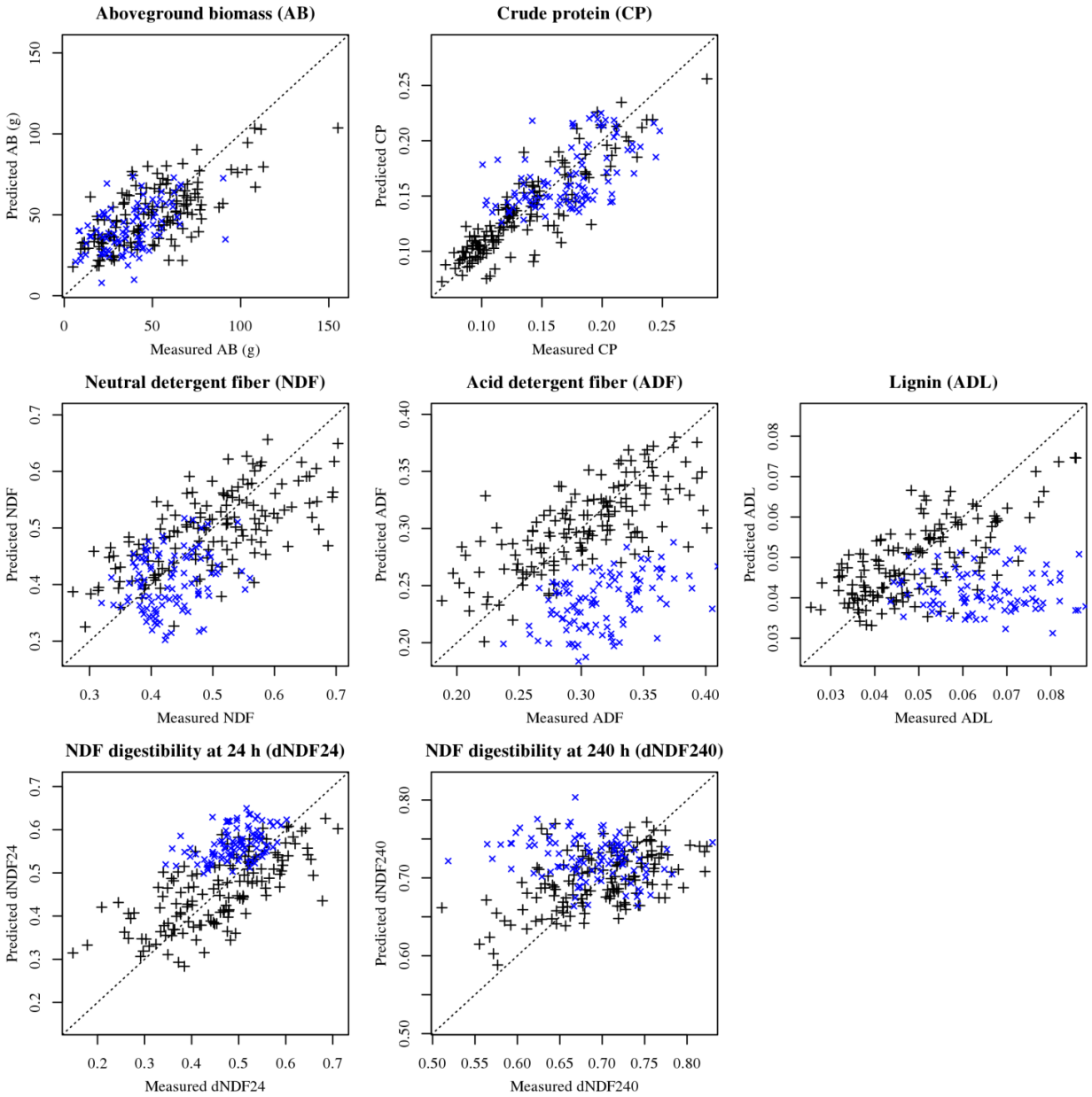

704
705 **Figure 6 – Predicted values of each variable compared to the measured ones. Values of 2012 dataset are marked with black**
706 **"+", 2013 ones with blue "×".**

707

Table 1 – Relative importance of models' predictors and adjusted R^2 (adj-R^2) of models. Column "model" indicates which of the calibration models has been used (with the numeration used in paragraph "Model development"). Next columns indicate the R^2 contribution among each predictor [Lindeman et al., 1980; Chevan and Sutherland, 1991] (signs between brackets refer to the sign of each coefficient in the regression). In columns "DOY/DOS" values refer to the predictor used in each model ("DOY" if model 1 or 2, "DOS" if model 3).

Y	Model	BGS	NDVImax	aspectNS	NDVI	DOY/DOS	DOY/DOS^2	NDVI:DOY/DOS	NDVI:DOY/DOS^2	adj-R^2
AB	2	(–) 0.172	(+) 0.068	(+) 0.023	(–) 0.164	(+) 0.048	(–) 0.043	(+) 0.009	(+) 0.009	0.507
CP	3	(–) 0.060	(+) 0.070	(+) 0.017	(–) 0.046	(–) 0.378	(+) 0.233	(–) 0.005	(+) 0.007	0.804
NDF	1	(–) 0.021	(–) 0.171	(–) 0.012	(+) 0.015	(+) 0.249		(–) 0.011		0.457
ADF	1	(–) 0.143	(–) 0.075	(–) 0.003	(–) 0.017	(+) 0.314		(+) 0.003		0.535
ADL	2	(–) 0.154	(+) 0.052	(+) 0.002	(–) 0.061	(+) 0.121	(–) 0.117	(–) 0.019	(+) 0.019	0.519
dNDF24	1	(+) 0.061	(+) 0.016	(+) 0.001	(–) 0.013	(–) 0.442		(+) 0.001		0.513
dNDF240	1	(+) 0.041	(–) 0.047	(–) 0.022	(+) 0.057	(–) 0.178		(–) 0.012		0.329

709 **Table 2 – Univariate analysis of variance between each experimental variable and pure NDVI values. *t* test coefficients and**

710 **their *p* values refer to NDVI predictor; R^2 values are also given.**

Y	*t* value	Pr (|*t*|)	R^2
AB	6.7	< 0.001	0.25
CP	–2.6	0.010	0.04
NDF	–1.2	0.225	0.00
ADF	1.5	0.124	0.01
ADL	4.3	< 0.001	0.11
dNDF24	–1.6	0.106	0.01
dNDF240	–4.0	< 0.001	0.09

711

Table 3 – Validation metrics (RMSE, MAE, NRMSE and NMAE, see paragraph *Model validation*) computed for each model and for each validation dataset (2012 with cross-validation and 2013). ΔY values summarise the distributions of the differences between measured and predicted values (as mean ± standard deviation), in order to estimate the presence of biases.

Y	RMSE 2012	RMSE 2013	MAE 2012	MAE 2013	NRMSE 2012	NRMSE 2013	NMAE 2012	NMAE 2013	ΔY 2012	ΔY 2013
AB	19	16	15	13	0.13	0.11	0.10	0.09	0±19	–4±16
CP	0.02	0.03	0.02	0.03	0.09	0.14	0.07	0.11	0.00±0.02	0.00±0.03
NDF	0.08	0.07	0.06	0.06	0.18	0.16	0.14	0.13	0.00±0.08	0.03± 0.06
ADF	0.03	0.09	0.03	0.08	0.16	0.4	0.12	0.4	0.00±0.03	0.08± 0.03
ADL	0.009	0.03	0.007	0.03	0.15	0.5	0.12	0.4	0.000±0.009	0.026±0.015
dNDF24	0.08	0.09	0.06	0.07	0.14	0.16	0.11	0.13	0.00±0.08	–0.07±0.05
dNDF240	0.05	0.08	0.04	0.06	0.16	0.2	0.13	0.19	0.00± 0.05	–0.04±0.06

Supplementary material S1: estimation of BGS from NDVI time series

The procedure used to estimate the date of beginning of growing season (BGS) is here described. The aim is to identify a threshold relative value t of the maximal annual NDVI range which can be considered as the value corresponding to the start of grass growth. The method proposed by Fontana et al. [2008] was used; t was recomputed considering BGS as the day when the mean grass height (measured as described in paragraph *Field data*) exceeds the value of 5 cm. To compute this value, our 2012 field time series were interpolated with a spline to obtain daily values, as done for NDVI. Only 11 of 19 plots were used (in the 8 rejected plots, mean grass height was already greater than 5 cm in the first sampling). For each of the possible t thresholds (the 99 percentiles of each NDVI range), the days d_t when seasonal series reached t were computed. To avoid the influence of false detection in not meaningful period (winter), the first 100 days of the solar year were not considered. Then the difference between BGS and each d_t was analysed in terms of days of offset (OD) and adjusted R^2, calculated as showed in equations [S1-1] and [S1-2], where BGS_j and d_{tj} are the values of BGS and d_t in each plot j, and RSS_t and TSS_t are respectively the residual sum of squares and the total sum of squares of the linear regression between d_t and BGS.

$$OD_t = \frac{1}{n_{plot}} \sum_{j=1}^{n_{plot}} \left(d_{tj} - BGS_j \right) \quad [S1\text{-}1]$$

$$\text{adj-}R^2 = 1 - \frac{n_{plot} - 1}{n_{plot} - 2} \frac{RSS_t}{TSS_t} \quad [S1\text{-}2]$$

The method resulted efficient, allowing both to select the best threshold value ($t = 0.51$) and to well estimate the field measured BGS date (adj-$R^2 = 0.84$).

Figure S1-1 shows, for each possible value of t, the offset days (OD_t) and the adjusted R^2 values (adj-R^2_t). The lowest absolute OD has been obtained with $t = 0.51$ (with this value of t $OD_t = 0$), which was then selected as best threshold value.

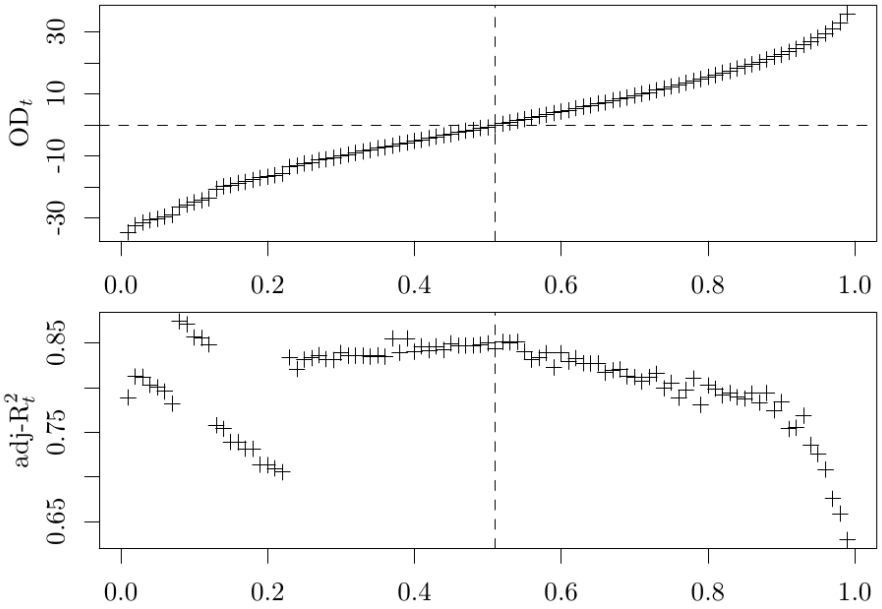

Figure S1-1 – Estimation of the NDVI threshold to use as BGS: OD (offset days) and adj-R^2 computed for each threshold value.

To check that this threshold is not only unbiased but also a good estimator of BGS, the adjusted R^2 was calculated as described in paragraph *Model development*. With $t = 0.51$ we obtained adj-$R^2 = 0.84$, which is one of the highest obtained with all the possible threshold values (Figure S1-1), justifying the use of $t = 0.51$ in the subsequent analyses.

Supplementary material S2: seasonal trends (2012) of field variables

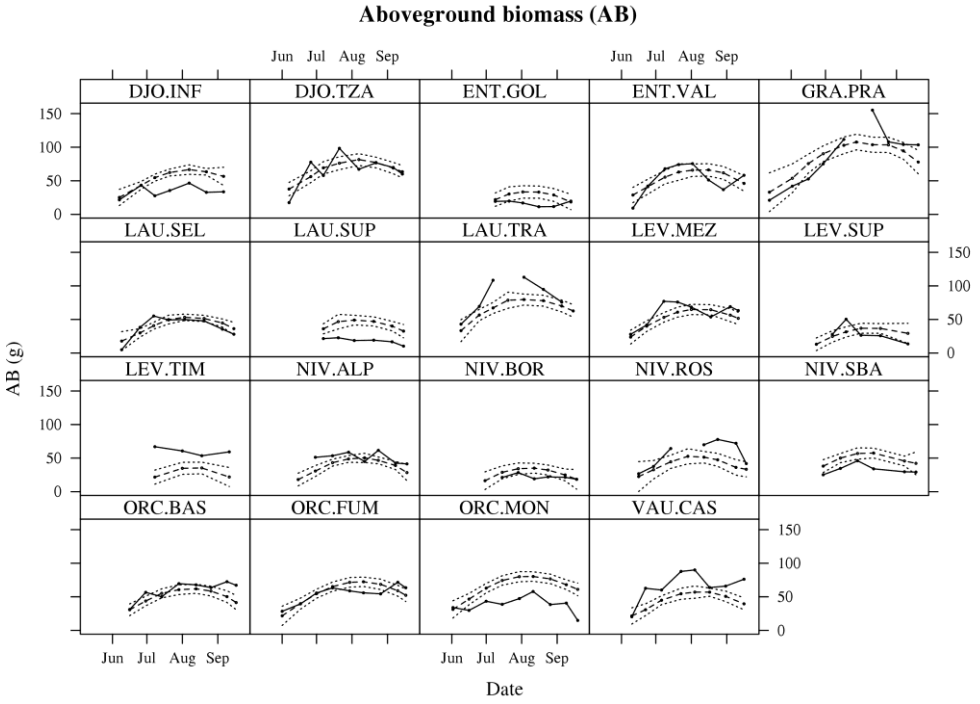

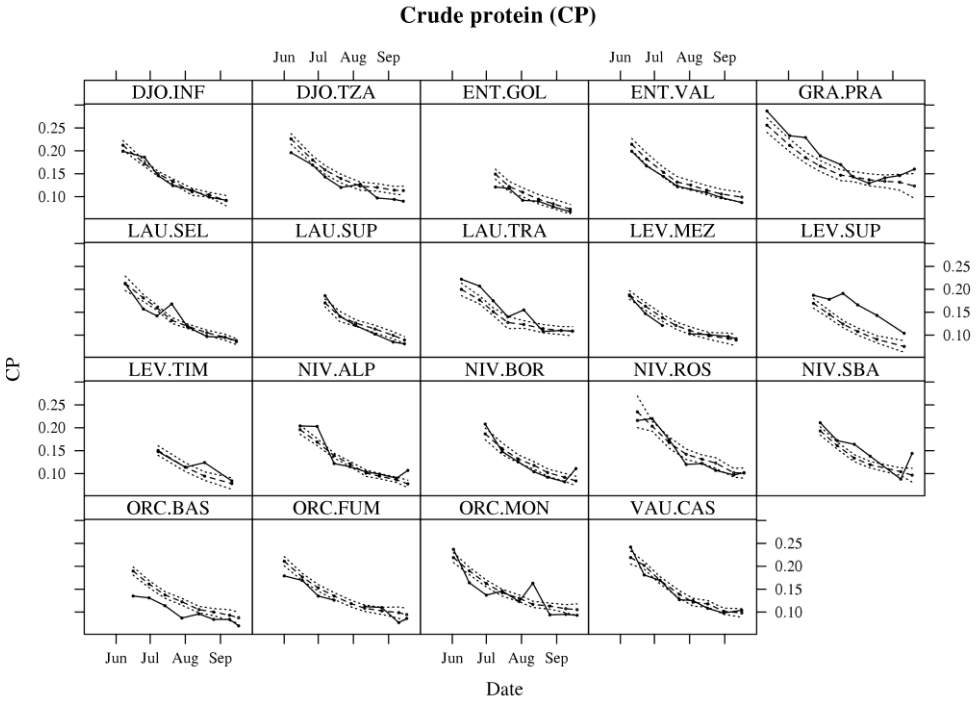

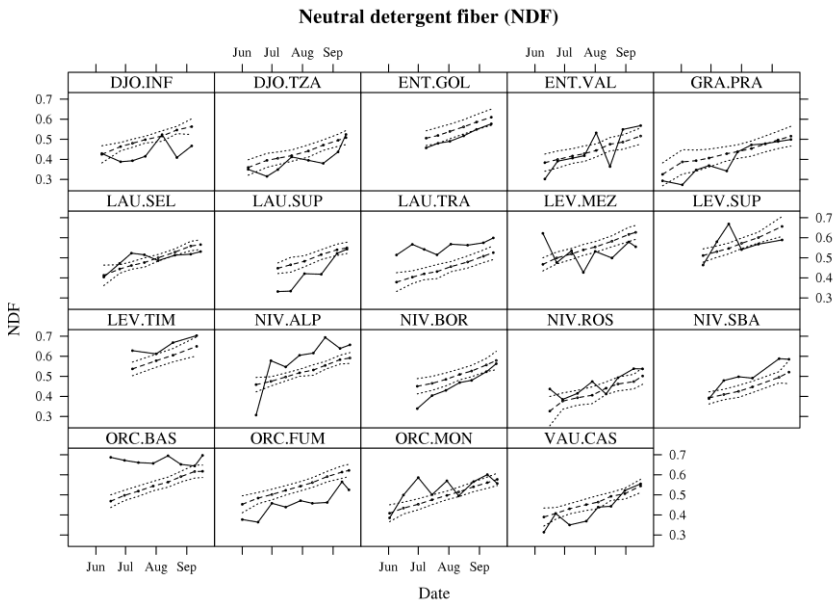
Neutral detergent fiber (NDF)
DJO.INF
DJO.TZA
ENT.GOL
ENT.VAL
GRA.PRA
LAU.SEL
LAU.SUP
LAU.TRA
LEV.MEZ
LEV.SUP
LEV.TIM
NIV.ALP
NIV.BOR
NIV.ROS
NIV.SBA
ORC.BAS
ORC.FUM
ORC.MON
VAU.CAS
NDF
Jun Jul Aug Sep
Date

747

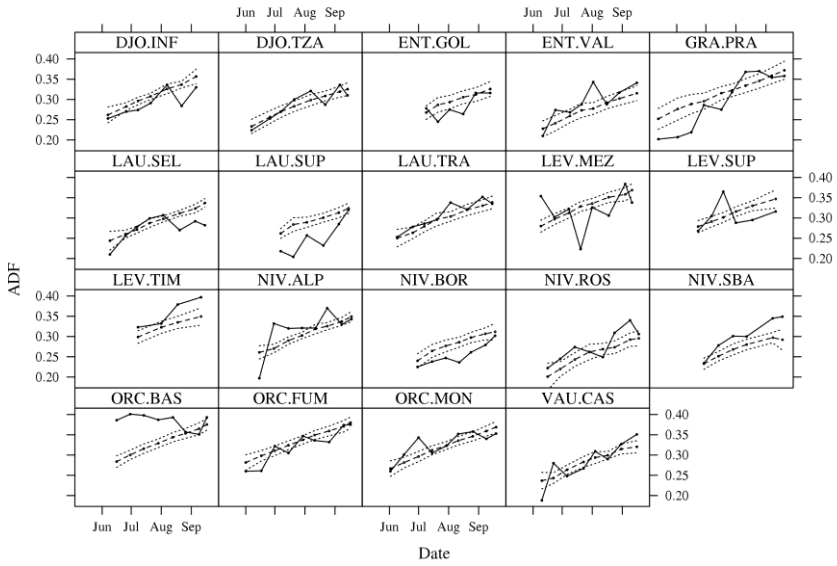
Acid detergent fiber (ADF)
DJO.INF
DJO.TZA
ENT.GOL
ENT.VAL
GRA.PRA
LAU.SEL
LAU.SUP
LAU.TRA
LEV.MEZ
LEV.SUP
LEV.TIM
NIV.ALP
NIV.BOR
NIV.ROS
NIV.SBA
ORC.BAS
ORC.FUM
ORC.MON
VAU.CAS
ADF
Jun Jul Aug Sep
Date

748

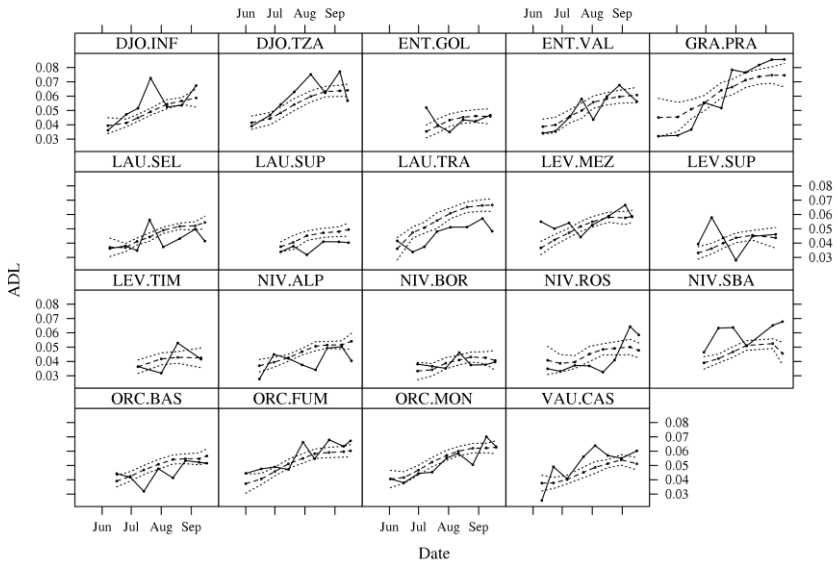
Lignin (ADL)
DJO.INF
DJO.TZA
ENT.GOL
ENT.VAL
GRA.PRA
LAU.SEL
LAU.SUP
LAU.TRA
LEV.MEZ
LEV.SUP
LEV.TIM
NIV.ALP
NIV.BOR
NIV.ROS
NIV.SBA
ORC.BAS
ORC.FUM
ORC.MON
VAU.CAS
ADL
Jun Jul Aug Sep
Date

749

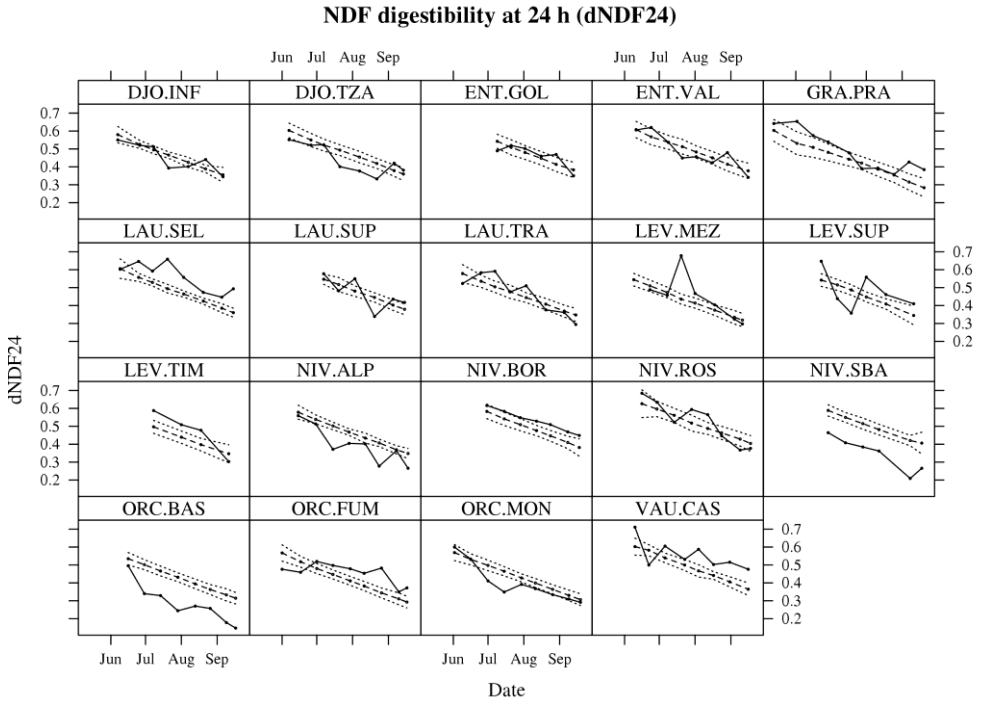

750

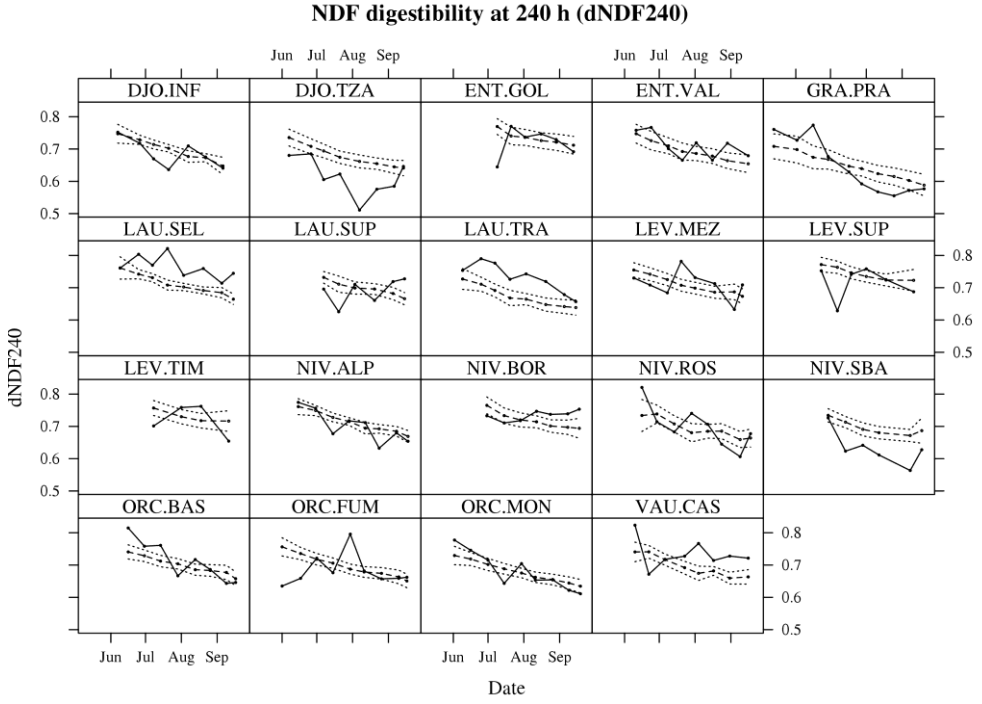

751

752 **Figure S2 – Seasonal trends (2012) of field variables. Solid lines represent the field measures, dashed lines represent**

753 **predicted values, dotted lines border 95% confidence intervals.**